Desalination and Water Treatment
www.deswater.com
doi: 10.5004/dwt.2022.28731

269 (2022) 269–283
September

Spatiotemporal differentiation of the water purification services in the basin of two karst lakes and one reservoir from the perspective of land use/cover changes

Wei Li[a], Linjiang Yin[a], Zulun Zhao[a], Weiquan Zhao[a,b,*]

[a]*Institute of Mountain Resource, Guizhou Academy of Sciences, Guiyang 550001, China, email: ZhaoWQ_2021@126.com (W. Zhao)*
[b]*School of Karst Science, Guizhou Normal University, Guiyang 550001, China*

Received 23 December 2021; Accepted 18 July 2022

ABSTRACT

Studying the differences in water purification services under land use/cover changes at different spatiotemporal scales is of great significance. The basin of Hongfeng Lake, Baihua Lake, and Aha Reservoir (referred to as two lakes and one reservoir) in Guiyang City is an important economic development area in the middle reaches of the Wujiang River, so human activities may affect the water quality of this area in a variety of ways. Based on the land use data in 2000, 2010, and 2020, the integrated valuation of ecosystem services and tradeoffs (InVEST) model was applied to simulate the spatiotemporal patterns of total nitrogen export and total phosphorus export from the basin of two lakes and one reservoir and quantitatively revealed the response relationship between land use changes and water purification services. Through multiangle analysis, the ecological and hydrological processes in the basin of two lakes and one reservoir are revealed to some extent, and the research results can provide a scientific basis for the optimization and adjustment of land use patterns, water quality protection, water pollution control, and measures for water ecological restoration in the basin of two lakes and one reservoir.

Keywords: InVEST model; Spatiotemporal differentiation; Two lakes and one reservoir; Water purification

1. Introduction

Land use/cover change is one of the main factors causing regional ecosystem service changes and material and energy flows and is the main cause of global warming, shrinkage of natural resources, and accelerated loss of biodiversity [1,2]. Studies have shown that land use/cover change is an intuitive reflection of human activities on the surface space and has become the main driver of global ecological and environmental problems [3–5]. Since the 21st century, the degradation of ecosystem services in China has led to a series of problems, such as the shortage of regional water resources and the decline in the quality of water ecosystems, severely restricting regional sustainable development [6–8]. Studies have found a significant correlation between land use/cover change and regional water ecosystem services [9–11]. On the one hand, the excessive reclamation of land resources and mining have reduced forest vegetation resources and changed soil texture, resulting in less absorption and transformation of nutrients such as nitrogen (N) and phosphorus (P) by vegetation and soil and more retaining of nutrients in the surface environment. On the other hand, the excessive use of N, P, and other farmland fertilizers causes nutrients to flow into the water bodies through rainfall runoff and thus increases the concentration of nutrients in the aquatic

* Corresponding author.

environment, which results in the destruction of the original physical and chemical structures of the aquatic environment and the degradation or even extinction of aquatic biodiversity, inevitably leading to the accelerated loss of regional water ecosystem services [12]. Earlier water quality monitoring and evaluation and point source pollution control and management measures can no longer solve the problem of water environment deterioration caused by economic development, whereas the response relationship between regional land use/cover and water quality, which is closely related to the control of nonpoint source pollution, needs to be addressed to solve the problem. Therefore, studying the pollution migration patterns in the context of land use/cover change at the basin scale has become the key to the scientific management of basins [13].

As an important component of ecosystem services, water purification in the context of land use/cover change is a topic of major interest in ecological research and has attracted the attention of many scholars [14,15]. In terms of research on pollutant loads in water environments, high-accuracy estimation of the overall pollutant load in a basin can be achieved by establishing a small-catchment test site and measuring the N and P loads of nonpoint source pollutants in the test site, but this method is time-consuming and laborious, so it is not suitable for large-scale research [16,17]. Export coefficient methods, empirical models, and process mechanism models are commonly used to simulate loads of pollutants such as N and P at the basin scale [18]. For example, Wang et al. [19] used a dynamic export coefficient model to simulate the nonpoint source pollution in a reservoir area and found sensitive areas of nonpoint source pollution. Wang et al. [20] proposed a simple and reliable empirical model to assess the nonpoint source pollutant load in the Chaihe Reservoir, where observational data was lacking, and found that both N and P excessively present in this region. In terms of land use/cover and water purification at the basin scale, Shen et al. [21] studied the relationship between water quality and land use/cover in the North Canal area and found that forestland and arable land were closely related to regional water quality and that forestland had a promoting effect on the quality of the water environment. Beckert et al. [22] found that different types of land use had different correlations with nonpoint source pollutant load and that the impact of arable land on total nitrogen (TN) was most notable. Piaggio and Siikamäki [23] found that forest mulch not only minimized soil erosion but also improved the quality of surface water by reducing and trapping sediments in the water. The export coefficient methods have low requirements in terms of input data, are not sensitive to scale, and have good portability. However, these methods do not consider migration and transformation processes, so their simulation accuracies are moderate. The process mechanism models consider the pollutant generation and migration processes, so they clearly show the mechanisms and processes and have high accuracy and portability. However, these models require a large number of parameters, a high data volume, and high data accuracy. In addition, few past studies have investigated the response relationship between mountainous areas with complex climates and topographies and water purification services or the response relationship between different land use types and water purification services. This study analyzed the heterogeneity of water purification services on different temporal and spatial scales, which is conducive to deepening the research on water purification services in the context of land cover changes.

The basin of Hongfeng Lake, Baihua Lake, and Aha Reservoir (referred to as two lakes and one reservoir) in Guiyang City is located in a typical karst landform area, with abundant water resources and intertwined river networks. Due to the characteristics of karst aquifers, surface water storage and water supply in this region are difficult, and most of the surface water flows into underground rivers and karst caves through karst seepage during the confluence process, resulting in a serious engineering water shortage and a strong dependence on surface water resources [24]. Due to more intense human activities and urban expansion in the past 20 y, a series of ecological and environmental problems, such as regional vegetation deterioration, rocky desertification and soil erosion, and groundwater pollution, still exist. The unique binary water structure system connecting the surface and underground is susceptible to connected pollution, so if water pollution incidents occur in this region, they are extremely difficult to control [25]. The integrated valuation of ecosystem services and tradeoffs (InVEST) model is widely used in the evaluation of ecosystem services. The parameter data required by the nutrient delivery ratio (NDR) model of the InVEST model are relatively easy to obtain, and the mechanism of the InVEST model is clear, so the InVEST model is suitable for the simulation of large-scale nonpoint source pollution. Therefore, carrying out research on water purification in this region is of great scientific significance. In summary, this paper uses the basin of two lakes and one reservoir as the study area and the subbasins as the assessment units to investigate the spatiotemporal differentiation pattern of water purification in the basin in the context of land use/cover change, with a view to provide a scientific basis for water pollution control and water ecological restoration measures in basins in southern China.

2. Overview of the study area

The basin of two lakes and one reservoir (105°51′–107°11′E, 26°9′–26°49′N) is located in the middle of the Wujiang River Basin, the largest tributary of the Yangtze River. The basin covers an area of 3,759.10 km^2 of Guiyang City, including Baiyun District, Yunyan District, Nanming District, Huaxi District, Qingzhen City, Gui'an New District, and some areas of Pingba District. The basin is high in the west and low in the east. The landform is dominated by inland karst mountains and hills. The mean elevation is approximately 1,200 m, the annual mean temperature is between 14°C and 16°C, and the mean annual precipitation is between 860 and 1,400 mm. The precipitation is mainly concentrated in summer, and the annual and seasonal precipitation has heterogenous spatiotemporal distributions. The two lakes and one reservoir provide 60% of the urban water use in Guiyang, so protecting the ecological environment of this region is extremely important. Over the years, industrial development, agricultural production, and domestic use around the basin have caused a sharp increase in the

water environment pressure in the basin, which has seriously threatened the sustainable development of the water ecosystem service of the two lakes and one reservoir.

3. Materials and methods

3.1. Data sources

The data obtained in this study consisted of four parts: (1) meteorological data, which were sourced from the China Meteorological Data Service Center (http://cdc.nmic.cn/), including data from 2000, 2010, and 2020 from the 20 meteorological stations around the study area, (2) digital elevation model (DEM) data with a spatial resolution of 30 m, derived from the geospatial data cloud (http://www.gscloud.cn/); (3) land use data of 2000, 2010, and 2020 interpreted from Thematic Mapper (TM) images (1:100,000), including 6 land use types, arable land, forestland, grassland, water, construction land, and unused land, as well as 25 secondary land use types, obtained from the Geographical Information Monitoring Cloud Platform (http://www.dsac.cn/), and (4) basic geographic data, including the administrative division of the study area, river systems, etc. All types of data were clipped using the vector boundary of the study area at the spatial resolution of 30 m and were all uniformly converted to WGS84/Albers Equal Area Conic projection for spatial calculation.

3.2. Research methods

3.2.1. Basin division

The basin range and subbasin boundaries of the study area were divided mainly by using the ArcGIS hydrological analysis tool. A total of 58 subbasins were segmented. The subbasins were used as the statistical units of the TN and total phosphorus (TP) export of the InVEST model at the basin scale.

3.2.2. Meteorological interpolation using AUNSPLIN software

The spatial distribution of rainfall in the basin is of great significance to the hydrological simulation of the basin. The topography of the basin of two lakes and one reservoir is complex, with an elevation difference of more than 700 m. Valleys are widely distributed in the mid-stream and downstream regions of the basin. The climate in the basin has high spatial heterogeneity, and the precipitation in the basin has high spatiotemporal heterogeneity. Conventional meteorological interpolation methods produce large errors [26,27]. Relevant studies have shown that the AUNSPLIN meteorological interpolation method has higher accuracy than traditional meteorological interpolation methods such as cokriging, inverse distance weighting (IDW), and kriging [28,29]. Therefore, this study introduces the topographic factor as a covariate for precipitation interpolation through AUNSPLIN software based on ordinary thin-plate and local thin-plate spline interpolation methods. The correlation statistical relationship between the meteorological factors and the longitudes, latitudes, and covariable (elevation) of the meteorological stations are established to simulate and calculate the values of meteorological factors at all grid points in the space of the study area, and the calculation formula is as follows:

$$Z_i = f(x_i) + b^n y_i + e_i \quad (i = 1\ldots\ldots N) \tag{1}$$

where Z_i is the dependent variable at point i in the space, $f(x_i)$ is an undetermined smooth function of x_i, x_i is an independent variable, y_i is a p-dimensional independent covariate, b is a p-dimensional coefficient of y_i, and e_i is the random error. $f(x_i)$ and b can be determined by the minimization of Eq. (2), namely, the least squares estimation:

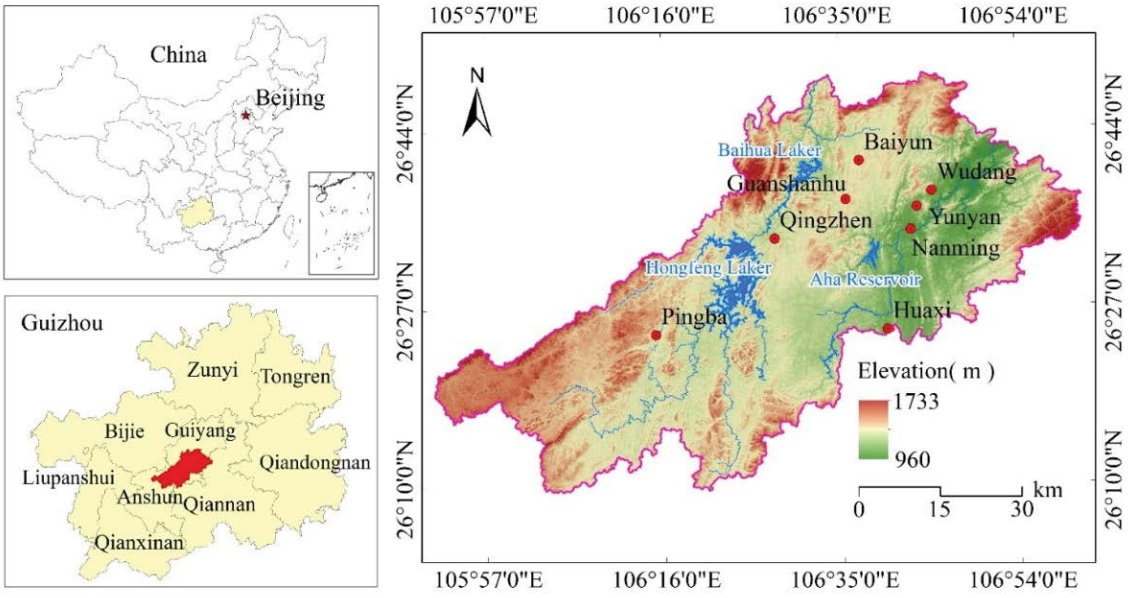

Fig. 1. Geographic location of the study area.

$$\min = \sum_{i=1}^{N}\left(\frac{z_i - f(x_i) - b^n y_i}{w_i}\right)^2 + \rho j_m(f) \tag{2}$$

where $j_m(f)$ is the roughness measurement function of the measurement function $f(x_i)$ also called the complexity function; m is the spline order in AUNSPLIN; ρ is a positive smoothing parameter (as ρ infinitely approaches to 0, the fitted interpolation becomes more accurate, and the function is infinitely close to the true value; as ρ approaches infinity, the fitted function approaches a least squares polynomial, and the order of the polynomial is determined by the order of the roughness penalty, m. The value of the smoothing parameter ρ is generally determined by minimizing the predictive error of the fitted surface (MSE) given by the generalized cross-validation (GCV) or determined by the generalized maximum likelihood (GML) estimation [30]. The optimal spatial interpolation models for precipitation selected in this study are all ternary splines with longitude, latitude, and elevation as independent variables, as shown in Fig. 2.

3.2.3. InVEST model

The InVEST model is a surface cover-based ecosystem service evaluation model jointly developed by the Woods Institute for the Environment of Stanford University, the Worldwide Fund for Nature, and The Nature Conservancy [31]. In this study, the water purification module in the InVEST model was used to analyze the spatial transport process of TN and TP to rivers, lakes, and reservoirs after TN and TP enter the surface of the basin from the outside world and to characterize the capacity of TN and TP retention and the migration process and pattern of TN and TP under different surface cover conditions. The formula for the nutrient export in water purification in the model is as follows:

$$X_{\text{expitot}} = \sum_i X_{\text{expi}} \tag{3}$$

$$X_{\text{expi}} = \text{load}_{\text{surf},i} \cdot \text{NDR}_{\text{surf},i} + \text{load}_{\text{subs},i} \cdot \text{NDR}_{\text{subs},i} \tag{4}$$

where X_{expi} is the nutrient export of each grid unit i in the basin, $\text{load}_{\text{surf},i}$ is the load of surface nutrients, $\text{NDR}_{\text{surf},i}$ is the surface nutrient delivery ratio, $\text{load}_{\text{subs},i}$ is the load of subsurface nutrients, $\text{NDR}_{\text{subs},i}$ is the subsurface nutrient delivery ratio, and X_{expitot} is the total nutrient export of the subbasins in the region.

(1) Formula for calculating the surface nutrient delivery ratio

$$\text{NDR}_i = \text{NDR}_{0,i}\left(1 + \exp\left(\frac{\text{IC}_t - \text{IC}_0}{k}\right)\right)^{-1} \tag{5}$$

$$\text{NDR}_{0,i} = 1 - \text{eff}_i' \tag{6}$$

$$\text{eff}_i' = \begin{cases} \text{eff}_{\text{LULC}_i} \cdot (1 - s_i) & \text{if down}_i \text{ is a stream pixel} \\ \text{eff}'_{\text{down}_i} \cdot s_i + \text{eff}_{\text{LULC}_i} \cdot (1 - s_i) & \text{if } \text{eff}_{\text{LULC}_i} > \text{eff}'_{\text{down}_i} \\ \text{eff}'_{\text{down}_i} & \text{otherwise} \end{cases} \tag{7}$$

$$s_i = \exp\left(\frac{-5\ell_{i_{\text{down}}}}{\ell_{\text{LULC}_i}}\right) \tag{8}$$

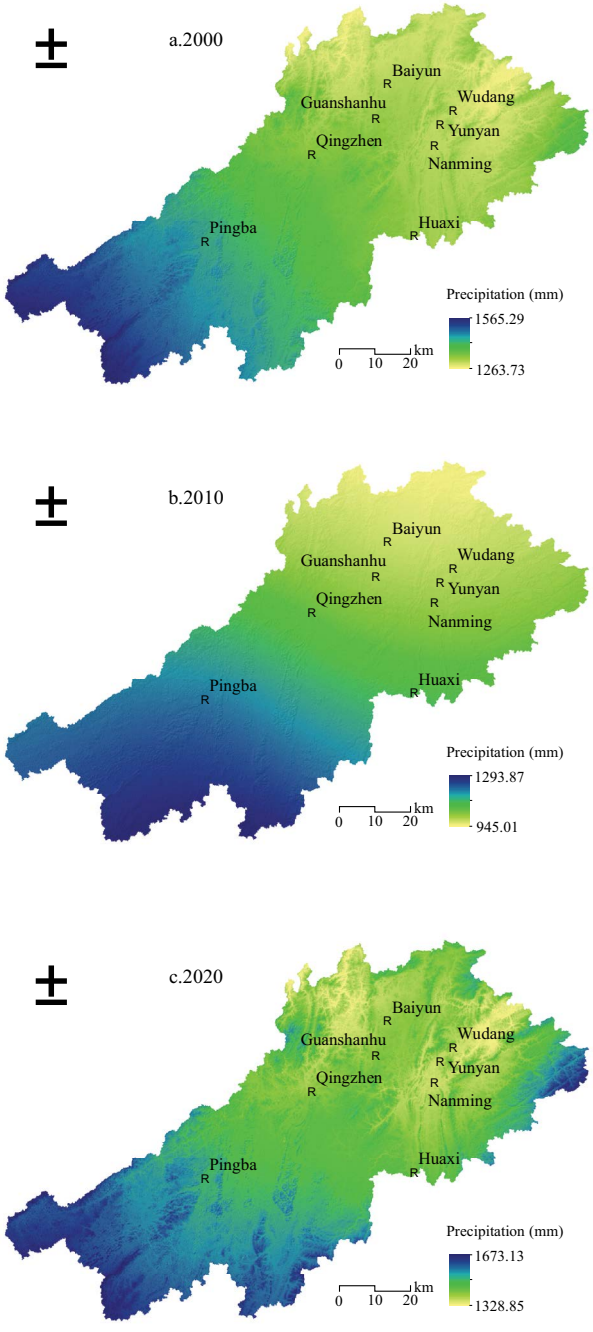

Fig. 2. Spatial distribution of precipitation in the basin of two lakes and one reservoir in 1995, 2000, 2010, and 2020.

$$\mathrm{IC} = \log_{10}\left(\frac{D_{\mathrm{up}}}{D_{\mathrm{dn}}}\right) \tag{9}$$

$$D_{\mathrm{up}} = \bar{S} - \sqrt{A} \tag{10}$$

$$D_{\mathrm{dn}} = \sum_i \frac{d_i}{S_i} \tag{11}$$

where $\mathrm{NDR}_{0,i}$ is the unreserved nutrient delivery ratio of the downstream grid unit, which is not related to the spatial location of the grid unit on the basin surface. IC_i is the regional topographic index; IC_0 and k are the correction coefficients; eff_i' is the maximum efficiency of nutrient retention in the surface grid unit i during nutrient transport from the surface grid unit to the river; $\mathrm{eff}_{\mathrm{LULC}_i}$ is the maximum efficiency of nutrient retention of land use type i during nutrient transport from the basin surface to the river; $\mathrm{eff}'_{\mathrm{down}_i}$ is the effective retention efficiency in the downstream grid unit i; s_i is the step size factor; $\ell_{i_{\mathrm{down}}}$ is the path distance from grid unit i to the adjacent grid in the downstream area of the basin; ℓ_{LULC_i} is the effective retention distance of the land use type of grid unit i; D_{up} is the mean slope gradient of the upslope area (m/m); A is the area contributed by the upslope area (m^2); d_i is the downslope flow path distance of the grid unit with the largest slope in grid unit i; and S_i is the slope gradient of grid unit i.

(2) Formula for calculating the subsurface NDR

$$\mathrm{NDR}_{\mathrm{subs},i} = 1 - \mathrm{eff}_{\mathrm{subs}}\left(1 - e^{\frac{-5\ell}{\ell_{\mathrm{subs}}}}\right) \tag{12}$$

where $\mathrm{eff}_{\mathrm{subs}}$ is the maximum retention efficiency of nutrients that can infiltrate into the ground from the surface grid units, l_{subs} is the retention length of the underground river, that is, the distance required for the soil to maintain the maximum capacity of nutrients, and l_i is the distance from grid unit i to the underground river.

The input parameters of the model include the DEM data (after filling the depression), land use type data, subbasin range, flow accumulation threshold of the basin, nutrient runoff proxy, N and P export loads and maximum N and P retention distances, vegetation retention efficiency, and Boreselli k parameter of the study area. The total annual rainfall in the study area was used as the nutrient runoff proxy. The flow accumulation threshold of the basin and the Boreselli k parameter were tested multiple times. Finally, the flow accumulation threshold of the basin was determined to be 500, and the Boreselli k parameter was set to 2. According to the similarity of the natural environment and referring to the InVEST model manual and the relevant research results [32–34], the values of the N and P export loading coefficients and vegetation retention efficiencies used in this study are shown in Table 1.

3.2.4. Pearson correlation analysis

In this study, using SPSS statistical software, the Pearson correlation coefficient was used to study the correlation between different land use types and water purification effects. The Pearson correlation analysis formula is as follows:

$$R = \frac{\sum_{i=1}^{n}\left(x_i - \bar{x}\right)\left(x_i - \bar{y}\right)}{\sqrt{\sum_{i=1}^{n}\left(y_i - \bar{x}\right)^2 \sum_{i=1}^{n}\left(y_i - \bar{y}\right)^2}} \tag{13}$$

where R is the correlation coefficient; $\bar{x}$ and $\bar{y}$ are the mean values of variables x and y, respectively; x_i and y_i are the ith observations of x and y, respectively; and n is the number of samples. R is between –1 and 1, and the larger the absolute value of R, the stronger the correlation between the land use type variable and the water purification variable. $R > 0$ indicates a positive correlation between the variables, and $R < 0$ indicates a negative correlation between the variables.

4. Result analysis

4.1. Characteristics of temporal and spatial changes in land use

Based on the spatial distribution of land use types in the basin of two lakes and one reservoir in 2000, 2010, and 2020 (Fig. 3) and statistical analysis of the data (Table 2), the overall land use patterns of the basin of two lakes and one reservoir showed the regional characteristics of arable land–forestland dominance from 2000 to 2020. The arable land occupied an absolute dominant position, followed by

Table 1
TN and TP loading coefficients and retention efficiencies

Land use types	Export loading coefficients of TN (kg hm^{-2} a^{-1})	Export loading coefficients of TP (kg hm^{-2} a^{-1})	Retention efficiencies of TN and TP
Arable land	24.2	5.75	0.25
Forestland	3.68	0.28	0.7
Grassland	8.5	0.55	0.4
Water	0.01	0.01	0.05
Construction land	14.5	3.85	0.05
Unused land	5	0.51	0.05

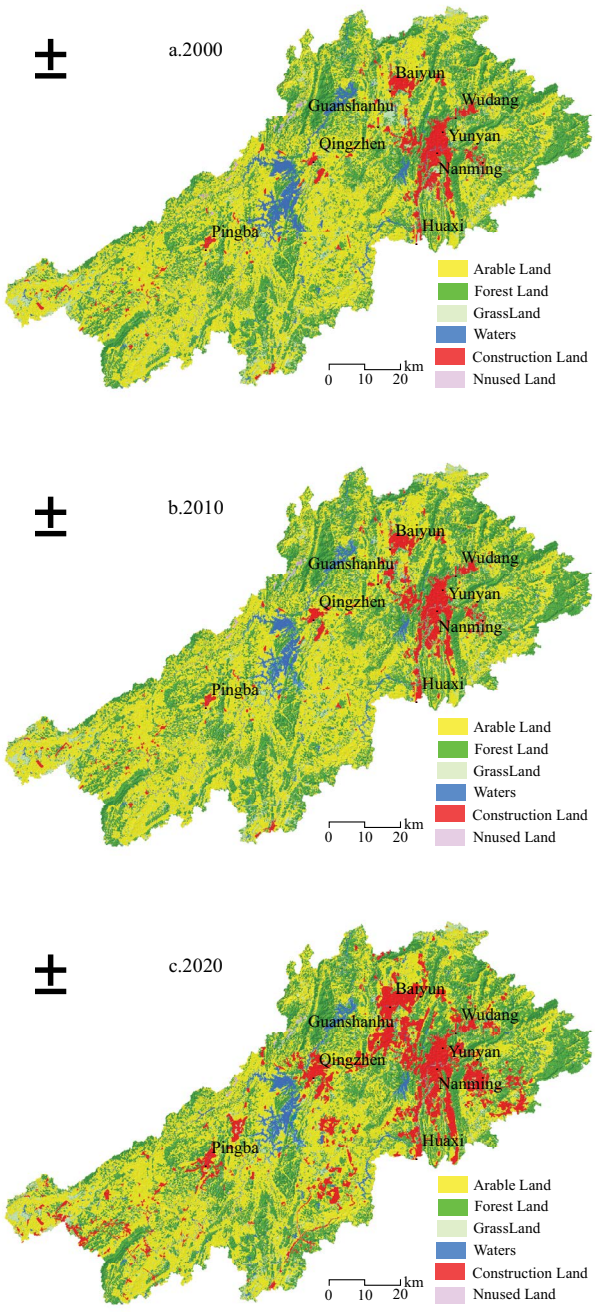

Fig. 3. Spatial distribution of land use types in the basin of two lakes and one reservoir in 1995, 2000, 2010, and 2020.

forestland, and unused land comprised the lowest proportion of the basin. Taking 2020 as an example, the total areas of arable land and forestland reached 1,687.81 and 1,335.23 km^2, respectively, accounting for 44.90% and 35.52% of the total area of the basin of two lakes and one reservoir. Most arable land was distributed in the areas with flat terrain west of Pingba District and those south of Qingzhen City, and the rest was scattered in the mountainous depressions and the hilly areas east of the main urban area. The forestland was mainly distributed in northern Qingzhen City, southern Pingba District, the eastern mountainous area of Yunyan District and Nanming District, and the surrounding forest parks of Guiyang City. Construction land was concentrated in the main urban area of Guiyang City in the downstream area of the basin, with a total area of 432.35 km^2, accounting for 11.50% of the total area of the basin.

From the perspective of the trend, the land use patterns of the basin of two lakes and one reservoir have undergone significant changes in the past 20 y. Except for the increase in the area of construction land, the areas of the land use types showed decreasing trends. The area of arable land decreased most prominently, with the area decreasing by 2.90 km^2 during 2000–2010 and by 182.47 km^2 (more rapidly) during 2010–2020. The area of forestland decreased the second most prominently, with the area decreasing by 34.87 km^2 during 2000–2020. The area of urban construction land increased notably, with the area increasing by 275.68 km^2 from 2000 to 2020 (432.35 km^2 in 2020), mainly to meet the demand for residential, industrial, and infrastructure land use. The area of urban construction land in 2020 was 2.76 times that in 2000, with a mean annual growth rate of 8.80% in 20 y. From the perspective of administrative division, the newly increased construction land was mostly distributed in the districts and cities of Guiyang City. The urban area of Pingba District extended to the urban area of Anshun City and Gui'an New District mainly because of the continuous acceleration of the urbanization process of Guiyang City and the continuous improvement in the socioeconomic level. In contrast, the area of water decreased by approximately 30.00% from 2000 to 2020, and the unused land decreased by 42.20%.

To analyze the conversion between various land use types in the basin in the past 20 y, transfer matrix analysis was performed based on the land use data from 2000, 2010, and 2020. The conversion between various land use types is shown in Table 3. The mutual transformation between various land use types is mainly manifested in the mutual transformation between arable land, forestland, and construction land. Of these land use types, arable land experienced the most dramatic changes, with a total decrease of 193.33 km^2 in 20 y. The decrease in arable land occurred because of agricultural structure adjustment and afforestation and the transformation of arable land to construction land. The newly increased construction land was mostly in the surrounding areas of the city mainly because the low-efficiency arable land in the surrounding areas of the city was transformed to construction land as a result of urban expansion and socioeconomic development. In addition, 116.84 and 48.89 km^2 of arable land were converted to forestland and grassland, respectively, mainly due to the implementation of the policy of returning farmland to forest and grassland and water source protection, which led to the transfer of unsuitable arable land to other land use types. Forestland was mainly converted to arable land, grassland, and construction land, including 109.74 km^2 converted to arable land, 58.01 km^2 converted to grassland, and 59.60 km^2 converted to construction land. Sparse shrubland and open forestland were the main types of forestland converted out. The areas of grassland and water also changed considerably. Specifically, a large area of grassland was converted to forestland, arable land, and construction

Table 2
Areas of and changes in each land use type in the basin of the two lakes and one reservoir from 2000 to 2020

Land use types	Areas (km^2)			Changes (km^2)		
	In 2000	In 2010	In 2020	2000–2010	2010–2020	2000–2020
Arable land	1,873.18	1,870.28	1,687.81	–2.9	–182.47	–185.37
Forestland	1,370.41	1,388.23	1,335.53	17.83	–52.7	–34.87
Grassland	267.31	267.99	239.88	0.68	–28.11	–27.43
Water	85.9	54.24	60.2	–31.67	5.96	–25.71
Construction land	156.67	173.53	432.35	16.85	258.82	275.68
Unused land	5.63	4.84	3.33	–0.79	–1.51	–2.3

Table 3
Land use transfer matrix of the basin of two lakes and one reservoir from 2000 to 2020 (km^2)

Years	Land use types	Arable land	Forestland	Grassland	Water	Construction land	Unused land
2000–2010	Arable land	1,705.66	109.99	45.33	9.19	2.84	0.17
	Forestland	100.41	1,198.04	61.9	6.81	2.59	0.66
	Grassland	51.98	63.49	134.96	13.75	3.01	0.12
	Water	5.72	12.45	21.88	0.35	45.5	0
	Construction land	5.76	3.66	3.52	143.43	0.3	0.01
	Unused land	0.75	0.6	0.4	0	0	3.88
2010–2020	Arable land	1,485.64	138.93	53.05	188.06	4.47	0.13
	Forestland	142.84	1,114.96	66.58	58.25	5.48	0.12
	Grassland	47.23	71.81	111.16	28.24	9.51	0.04
	Water	3.28	5.8	4.07	0.49	40.6	0
	Construction land	8.54	3.63	3.91	157.3	0.14	0.01
	Unused land	0.28	0.4	1.11	0.01	0	3.03
2000–2020	Arable land	1,509.44	116.84	48.89	193.33	4.51	0.17
	Forestland	109.74	1,139.45	58.01	59.6	3.51	0.1
	Grassland	52.6	62.66	109.73	39.14	3.13	0.05
	Water	6.19	12.02	18.05	0.81	48.83	0
	Construction land	8.98	3.65	4.41	139.43	0.19	0.01
	Unused land	0.86	0.91	0.79	0.04	0.03	3

land, and the water was mainly converted to grassland, forestland, and arable land. Construction land was mainly converted to arable land, forestland, and grassland. Due to the impacts of policies such as poverty alleviation relocation and ecological resettlement, old houses were demolished after relocation, and the land was then reclaimed or reforested. Overall, the change in construction land was mainly due to the conversion of other land use types into construction land, while the change in unused land was relatively stable.

4.2. Spatiotemporal distribution characteristics of water purification service

From a spatial perspective, the water purification service of the basin of two lakes and one reservoir had obvious spatial differences in 2000–2020. Within the basin, high TN and TP export intensities were mainly distributed in the area of Xinjiang River and Leping River in the upstream of the basin and around the subbasin (where the Hongfeng Lake is located) south of Qingzhen City in the mid-stream area of the basin. The minimum intensities of TN export all exceeded 6.70 kg hm^{-2}, and the minimum intensities of TP export all exceeded 1.20 kg hm^{-2}. The high TN and TP export intensities resulted from the use of N and P fertilizers in the large area of arable land around these regions. The low TN and TP export intensities were mainly distributed in western Baihua Lake, eastern Yunyan District, and eastern Nanming District. The maximum intensities of TN export were all below 3.70 kg hm^{-2}, and the maximum intensities of TP export were all below 0.62 kg hm^{-2}. The low TN and TP export intensities occurred because these regions were mainly covered by forestland, which has high absorption, transformation, and retention rates for nutrients such as N and P and thus reduces the intensities of N and P export. In terms of the entire basin, the downstream area had better water purification services than the mid-stream and upstream areas. The high TN and TP export intensities were mainly concentrated in areas with intensive agricultural activities, while the low TN and TP export intensities were

mainly concentrated in forestland with complete ecosystem services and fewer human activities, as shown in Fig. 4.

From a temporal perspective, the TN and TP export in the basin of two lakes and one reservoir exhibited differences in 2000, 2010, and 2020. The total export of TN increased from 1,927.87 t in 2000 to 1,939.98 t in 2010 and then decreased to 1,879.75 t in 2020. During the same period, TP also increased first and then decreased, with a total decrease of 2.44 t. The total TN and TP export changed only slightly. Therefore, 2020 was the year with the best water purification service in the basin. Overall, the TN and TP export intensities of the 58 subbasins did not change much during the 20 y from 2000 to 2020 (Table 4), and the overall TN and TP export showed a slow decreasing trend. Therefore, 2020 was the year with the best regional water purification services. The maximum and minimum values of TN and TP export per unit area all appeared in 2010. The maximum and minimum values of TN export intensity were 8.35 and 2.66 kg hm^{-2}, respectively, while the maximum and minimum values of TP export intensity were 1.30 and 0.38 kg hm^{-2}, respectively. The maximum values of TN and TP export intensities were more than 3 times the minimum values of TN and TP export intensities, respectively. In the 58 subbasins, the TN and TP export was not greatly different. From the perspective of the total export range of the subbasins, the TN export was mostly between 20 and 40 t, and 28 subbasins exported TN. The TP export was mostly between 2 and 6 t. The distribution of high TN and TP export did not change much between different years. From 2000 to 2020, the TN purification effect in the basin continuously improved, while the

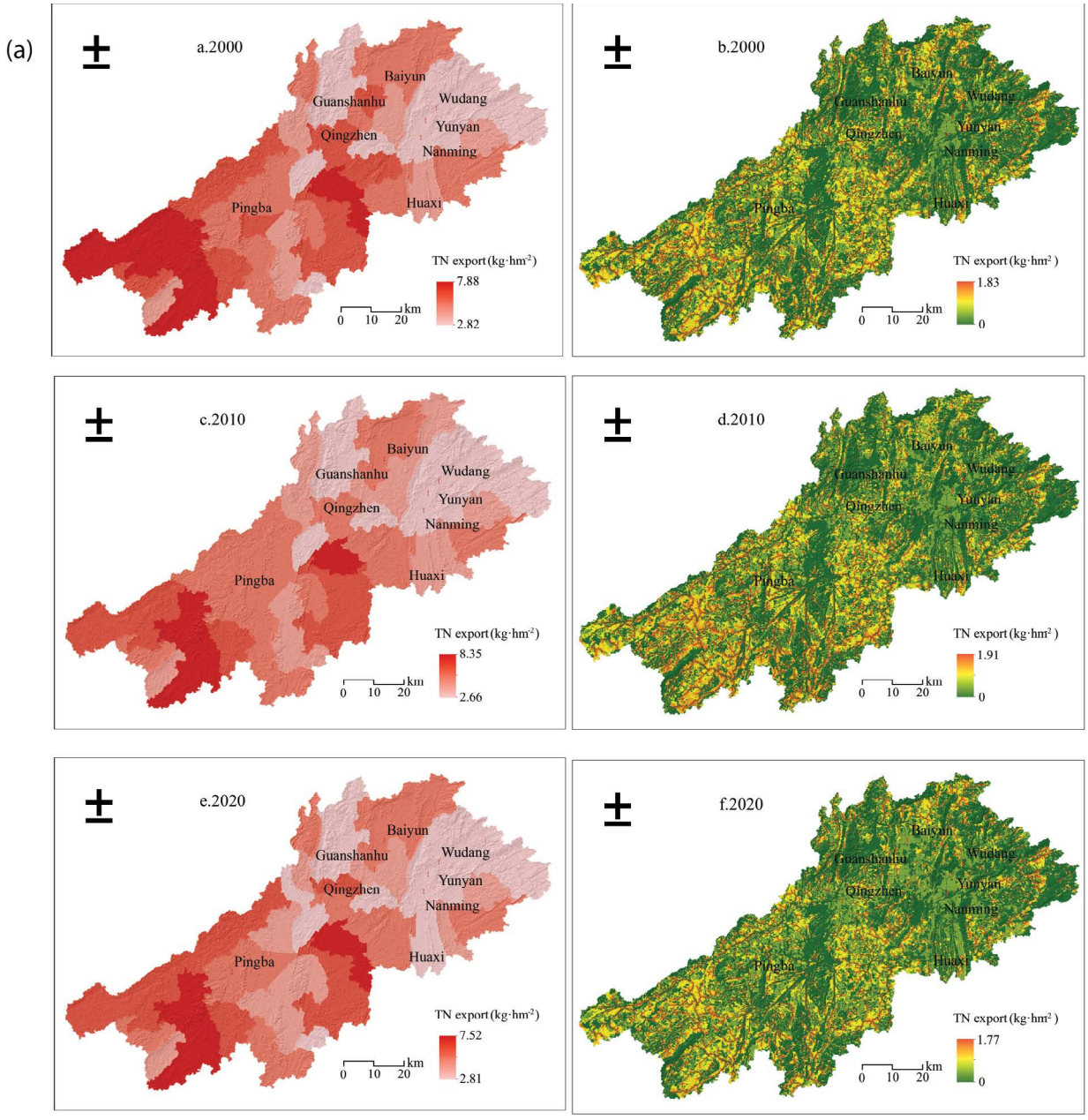

(Continued)

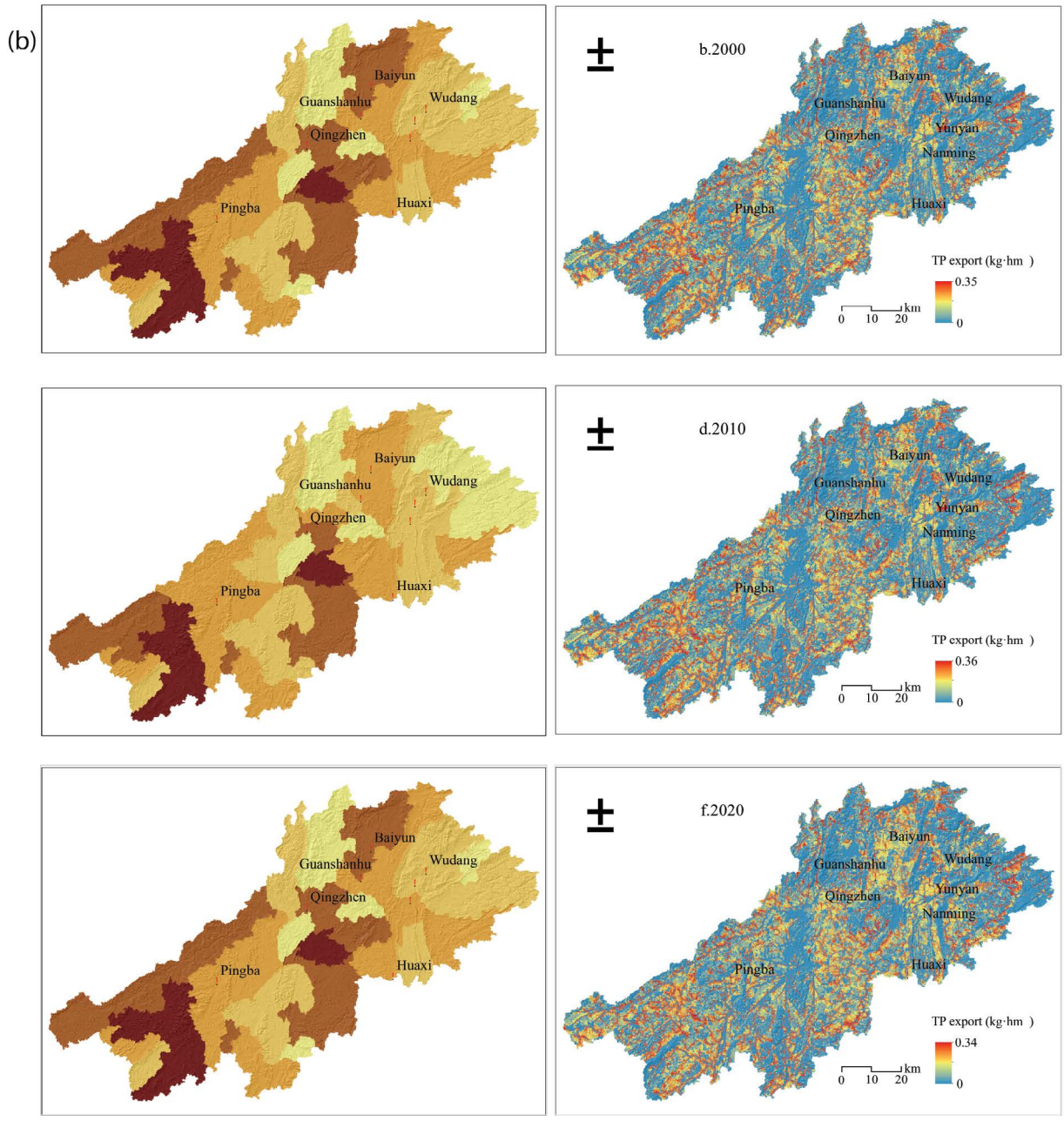

Fig. 4. Spatial distribution of (a) TN and (b) TP export in the basin of two lakes and one reservoir in 2000, 2010, and 2020.

TP purification effect in the basin fluctuated. Overall, the water purification service of the basin has been steadily improving.

4.3. Response relationship between land use type and TP and TN export

To reflect the impact of land use types in the basin on regional water purification, correlation analysis was performed between the areas of different land use types and the total TN and TP export in the basin of two lakes and one reservoir in 2000, 2010, and 2020 (Table 5). The correlation analysis results showed that the TN and TP export differed significantly between different land use types, that is, different land use types had different water purification services. From the perspective of the coefficients of correlation between the total TN and TP export and the land use types in each period, the total TN and TP export had strong correlations with arable land, forestland, and grassland but had weak correlations with water, construction land, and unused land. The correlations between the total TP and TN export and the arable land were the strongest, with correlation coefficients of 0.91 and 0.96, respectively, in 2020, followed by the correlation between the total TP and TN export and the grassland, with correlation coefficients exceeding 0.75 in 2020. The correlations between the

Table 4
Distribution of TN and TP export in the subbasins

Total export of TN	Number of subbasins			Total export of TP	Number of subbasins		
	In 2000	In 2010	In 2020		In 2000	In 2010	In 2020
<20 t	15	15	16	<2 t	2	3	2
20–40 t	30	28	29	2–4 t	19	19	19
40–60 t	10	12	10	4–6 t	21	16	20
60–100 t	1	1	1	6–10 t	13	17	14
>100 t	2	2	2	>10 t	3	3	3

Table 5
Correlation coefficients between the total TP and TN export in each subbasin of the basin of two lakes and one reservoir and each land use type from 2000 to 2020

Years	Land use types	Total export of TP	Total export of TN	Arable land	Forestland	Grassland	Water	Construction land	Unused land
In 2000	Total export of TP	1	0.99	0.96	0.51	0.77	0.03	0.14	0.11
	Total export of TN	0.99	1	0.98	0.52	0.76	0.057	0.06	0.1
In 2010	Total export of TP	1	0.99	0.96	0.49	0.77	0.01	0.11	0.02
	Total export of TN	0.99	1	0.98	0.49	0.78	0.04	0.02	0.01
In 2020	Total export of TP	1	0.98	0.91	0.51	0.75	0.03	0.34	0.19
	Total export of TN	0.98	1	0.96	0.53	0.78	0.07	0.2	0.19

total TP and TN export and unused land and the correlations between the total TP and TN export and construction land were weak. The total TP and TN export did not correlate with the water. These results indicate that the impact of ecosystem type on the water purification of the basin was related to the areas of different land use types and that arable land was the land use type most closely related to nonpoint source pollutant load.

Arable land, grassland, and forestland are the three land use types that strongly correlated with the total TN and TP export on the basin scale. Therefore, on the subbasin scale, the relationship between the total TN and TP export and the three land use types were analyzed (Fig. 4). The total TN and TP export had noticeable correlations with the area of the arable land. As the area of arable land reached the peak value, the TN and TP export also reached peak values; that is, the larger the area of arable land in the subbasin was, the larger the TN and TP export. As the area of forestland exceeded the area of arable land, the total TN and TP export decreased. Like arable land, as the area of grassland peaked, the TN and TP export also peaked. These results indicate that the TN and TP export under different land use types occurred in the descending order of arable land > grassland > forestland, while the water purification services were in the ascending order of arable land < grassland < forestland, as shown in Fig. 5.

Through the regression analysis of the total TN and TP export in each subbasin and each land use type, the total TN and TP export had linear relationships with the area of each land use type, and the regression equations are shown in Table 6. The linear relationships best fit the relationship between the total TN and TP export and arable land, with R^2 values of 0.83 and 0.92, respectively, followed by R^2 values (0.56 and 0.60, respectively) for the relationship between the total TN and TP export and grassland. The R^2 values for the relationship between total TN and TP export and forestland were 0.25 and 0.27, respectively. The R^2 values for the relationship between total TN and TP export and construction land were 0.12 and 0.03, respectively. The R^2 values for the relationship between total TN and TP export and unused land were 0.05 and 0.07, respectively. The R^2 values for the relationship between total TN and TP export and water were –0.014 and –0.008, respectively. Therefore, the area of arable land in the basin had the highest linear correlations with the total TN and TP export, and the areas of grassland and forestland had the second highest linear correlations with the total TN and TP export. The areas of construction land and unused land had low correlations with the total TN and TP export. The area of water had no obvious correlation with the total TN and TP export.

In summary, the total TP and TN export was affected by the area of arable land. The larger the area of arable land

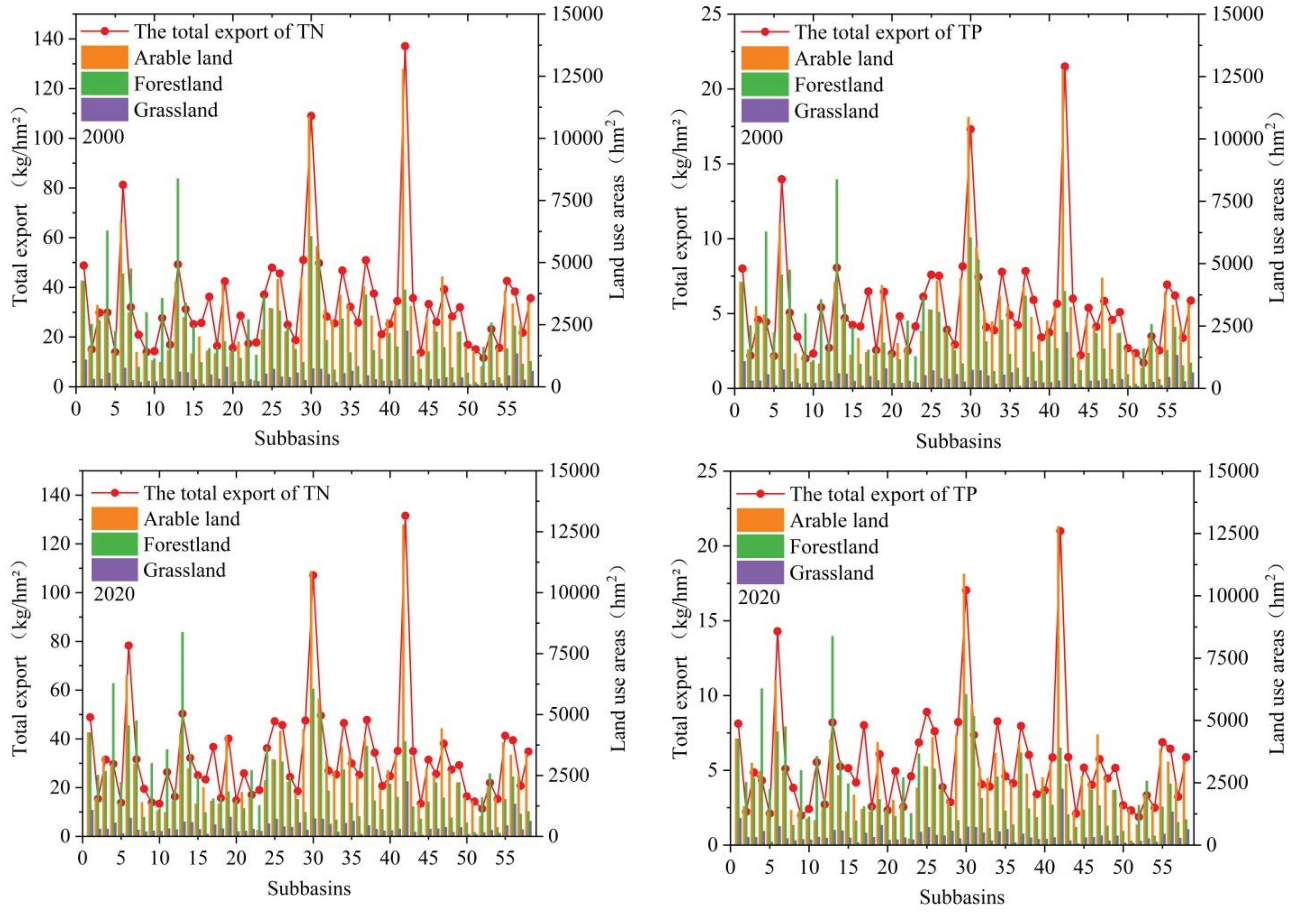

Fig. 5. Comparison of the areas of arable land, forestland, and grassland in the basin with the total TP and TN export (the abscissa represents the subbasins).

was, the greater the total TP and TN export, which further indicates that arable land is the main contributor to the worsening of water purification services. Grassland and forestland exhibit certain water purification services, while construction land and unused land have no notable effect on water purification.

5. Discussion

5.1. Factors affecting water purification in the basin of two lakes and one reservoir

The water environment quality of basins is controlled by the topography of basins, regional climate, ecological function structure, and human activities [35]. At present, studies on water ecosystem services in the basin of two lakes and one reservoir mainly measure the water environment health status by sampling water from the lakes and reservoir, and the accuracy of this method is high within the water but low in quantifying the water environment status and influencing factors at the basin scale [36–38]. With the continuous expansion of the scope of human activities, relevant scholars are paying increasing attention to the impact of environmental changes in the basin on the water quality in the region. This study applied the InVEST model to investigate the water purification in the two lakes and one reservoir. The greatest strength of the InVEST model lies in its capability to quantitatively reveal the nature of ecological and environmental problems in the basin [39]. The results of this study have truthfully revealed the spatiotemporal characteristics of water purification services in the basin and the response relationships between water purification services and land use over the past 20 y. The results of this study are consistent with those of previous studies [40].

The water purification services of forestland and grassland in the basin of two lakes and one reservoir were significantly better than those of other land use types. The main reason is that the areas with high vegetation cover, such as forestland and grassland, have lower runoff flow rates, so they have higher N and P export loading coefficients and vegetation retention efficiencies than other land use types, resulting in stronger absorption, retention, decomposition, and transformation and lower export intensities of nutrients such as N and P. Arable land is a land use type with high TN and TP export intensities in the basin, and the water purification services of arable land are the worst, mainly because the ecosystem of arable land is greatly affected by human activities. The heavy application of N and P fertilizers is the key factor causing the deterioration of water quality in the basin. Specifically, N fertilizers can be rapidly

Table 6
Regression equations for the total TP and TN export and land use types in the subbasins in 2020

Land use types	Total export of TP		Total export of TN	
	Regression equations	R^2	Regression equations	R^2
Arable land	$Y = 550.86X - 71.02$	0.83	$Y = 96.35X - 207.30$	0.92
Forestland	$Y = 234.30X + 1{,}028.77$	0.25	$Y = 40.41X + 989.34$	0.27
Grassland	$Y = 75.53X + 3.52$	0.56	$Y = 12.92X - 5.87$	0.6
Water	$Y = 3.60X + 84.28$	–0.014	$Y = 1.45X + 70.41$	–0.008
Construction land	$Y = 102.51X + 189.42$	0.12	$Y = 10.41X + 407.88$	0.03
Unused land	$Y = 1.43X - 2.01$	0.05	$Y = 0.27X - 2.96$	0.07

converted to nitrate nitrogen, P can easily bind with soil particles and other compounds, and the unabsorbed N and P flow into the lakes and reservoir with runoff. The policy of returning farmland to forest and grassland and the conversion of arable land to urban construction land have improved the water purification efficiency, resulting in spatial changes in regional water purification services.

In addition, from the perspective of water balance, the changes in climate factors such as precipitation, temperature, light, and radiation intensity cause changes in the vegetation cover of the underlying surface and the source, migration, and transformation of pollutants in the water environment [41,42]. Climate change and ecohydrological responses in karst regions are multiscale, nonlinear, complex spatial geoecological processes. It is difficult to accurately define and quantify the complex and variable environmental influencing factors and to observe and study the internal processes and control factors. In karst regions, nutrients such as P and N directly enter the groundwater system without the filtering effect of the soil layer and flow into the rivers, lakes, and reservoirs through underground rivers, which affects the water purification services of basins to a certain extent [43,44].

The analysis results of the water purification of the basin of two lakes and one reservoir based on the InVEST model objectively reflect the water purification services of the ecosystem in the entire region. Of course, this study has certain limitations. For example, the model parameters were selected and adjusted referring to the parameter settings in an existing study, resulting in a certain degree of subjectivity. Further improvement and discussion are needed to obtain high-accuracy data and to better set the model parameters.

5.2. Water environmental protection in the basin based on water purification

Land use and land use pattern have a significant impact on the water environment quality of the basin. According to the development plan of Guiyang City, the resident population in the region will reach 7 million in 2025. Since the two lakes and one reservoir are the main drinking water sources that support the strategy of strengthening the provincial capital of Guizhou, the population and water resource pressure in the downstream area of the basin will further increase. Relevant research results show that the water quality of Hongfeng Lake, Baihua Lake, and Aha Reservoir, the main drinking water sources in the basin of two lakes and one reservoir, has been in a mesotrophic state for a long time. Although the eutrophic level of the basin in recent years shows a decreasing trend, the eutrophic level is still high in some areas and has high heterogeneity in spatial distribution.

From the perspective of the contribution rates of land use types to the TN and TP export in the basin (Fig. 6 and Table 7), although the contribution rate of the arable land to TN and TP showed a decreasing trend from 2000 to 2020, the arable land still contributed 75% of the TN and TP export in the basin, followed by the contribution rates of construction land. Between 2000 and 2010, the overall contribution rates of land use types to TN and TP did not change significantly, and the changes in 2010–2020 were greater than those in 2000–2010. From 2010 to 2020, the contribution rates of land use types to TN and TP increased by 2.82 times and 2.22 times, respectively, mainly because the area of construction land increased by 258.82 km^2 from 2010 to 2020, which was 15.36 times the increase in the area of construction land from 2000 to 2010. The large-scale conversion of other land use types to construction land increased the runoff coefficient, resulting in poorer water purification services. Therefore, the contribution rates of land use types to TN and TP export increased rapidly between 2010 and 2020. The overall contribution rates of forestland to TN and TP were small. The contribution rate of forestland to TN TN was less than 0.45%, and the contribution rate of forestland to TP increased by 4.83% from 2000 to 2020. The contribution rate of grassland to TN remained basically unchanged, and the contribution rate of grassland to TP decreased by 1.46% from 2000 to 2020. The contribution rates of unused land and water to TN and TP in the entire basin were basically negligible. Due to the negative correlation between forestland/grassland and the water quality of the basin, the larger the area of forestland and grassland was, the smaller their contribution rates to TN and TP, and thus the stronger the water purification capacity.

According to the current land use statistics of the basin, the main land use types of the basin are arable land and forestland, and the sum of the area of the two accounts for 80.43% of the total area of the basin. The sum of the area of grassland, construction land, water, and unused land accounts for only 19.57% of the total area of the basin. Therefore, improvement in the water purification service

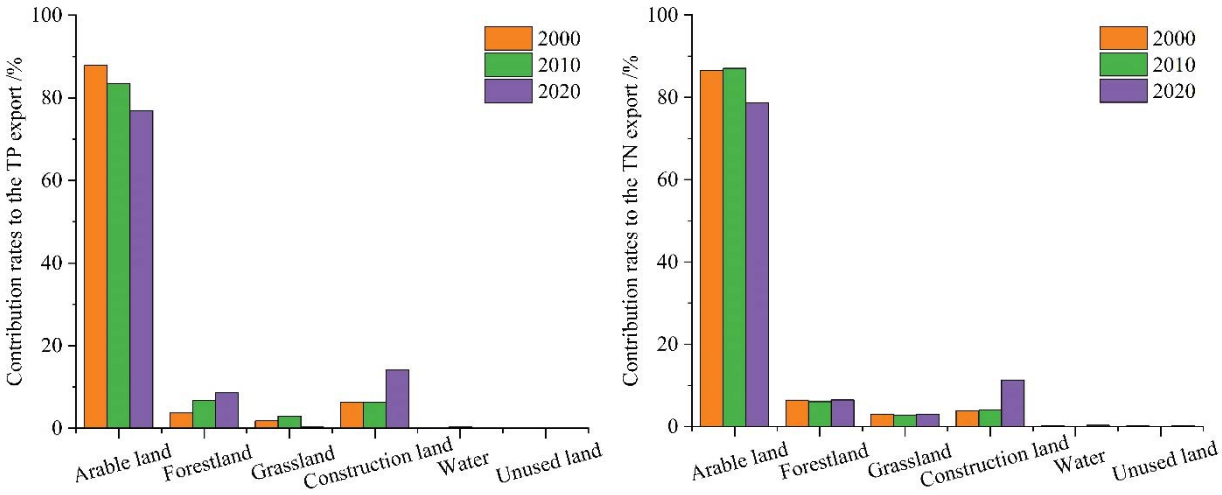

Fig. 6. Contribution rates of various land use types to the TP and TN export in the basin of two lakes and one reservoir from 2000 to 2020.

Table 7
Statistics of the contribution rates of various land use types to the TP and TN export in the basin of two lakes and one reservoir from 2000 to 2020

Land use types	Contribution rates to the TN export (%)			Contribution rates to the TP export (%)		
	In 2000	In 2010	In 2020	In 2000	In 2010	In 2020
Arable land	86.48	87.08	78.7	87.88	83.39	76.9
Forestland	6.31	6.04	6.49	3.78	6.78	8.61
Grassland	2.9	2.83	2.9	1.74	2.96	0.28
Water	0.19	0.03	0.32	0.2	0.31	0.07
Construction land	3.85	4	11.31	6.25	6.35	14.12
Unused land	0.15	0.02	0.28	0.15	0.2	0.02

in the basin mainly depends on arable land and forestland. In summary, improvement in water purification services in the basin of two lakes and one reservoir can be considered from the following aspects.

The previous analysis showed that the water quality of the basin was positively correlated with arable land and negatively correlated with forestland, grassland, and water, indicating that the wide distribution of forestland in a large area contributes to water purification of the basin. To control and improve the water quality of the rivers and reservoir of the basin, first, the proportion of forestland should be increased in the key areas, especially in the vicinity of drinking water sources in the mid-stream and downstream areas of the basin, such as Hongfeng Lake, Baihua Lake, and the area from the upstream of the Nanming River to Aha Reservoir, to improve the forest stand quality and to ensure vegetation cover. Second, the land use types should be reasonably allocated in areas within 100–200 m from the rivers and reservoir by maximizing the forestland and grassland cover and planting bioremediation plants in the riparian zones of the lakes and reservoir to increase plant biomass and to remove the N and P pollutants in soil as much as possible [45,46].

Arable land is the land use type that accounts for the largest proportion (44.90%) of the area of the basin, indicating that agricultural production activities are still dominant and that agricultural irrigation consumes large amount of water. The focus of the prevention and control of nonpoint source pollution in the basin is the area from both banks of the upstream Xinjiang River to the Hongfeng Lake area, the two banks of the Leping River in the north, the Pingba District between the Machang River and the Nanming River, and the upstream area of the Aha Reservoir. First, the proportion of arable land should be controlled, and fertilization should be scientifically applied to reduce its impact on water purification services and to improve the water purification effect of the overall ecosystem of the basin. Second, the project of returning arable land to forest and grassland should be implemented in areas such as sloping arable land, low-efficiency arable land, and areas close to drinking water sources, and the construction of ecological agriculture should be strengthened in low-altitude bar plains and hilly areas to promote the optimization of the land resource space of the basin. Third, the current agricultural industry structure should be adjusted to reduce the pollution of arable land to river water using measures such as vigorously

promoting modern ecological and efficient agriculture, increasing the yield per unit area of arable land, and reducing the dependence on large-scale arable land.

In addition, although construction land had no obvious correlation with water purification services in the entire basin, the contribution rates of construction land to the TN and TP export in 2020 both exceed 10%, and the production and convergence of pollutants in construction land cannot be ignored. Urbanization is still the major human activity in the basin. First, the horizontal expansion of construction land should be strictly controlled, and the vertical expansion of construction land should replace the horizontal expansion. Second, afforestation in construction land should be promoted, more parks and green space networks dominated by arbores and shrubs should be constructed, and the water permeable area inside the construction land should be increased to alleviate the pressure of the basin in water purification.

6. Conclusion

In this study, the basin of two lakes and one reservoir was used as the study area to quantitatively evaluate the water purification services of the basin by simulating the N and P export. The results reflected the characteristics and spatial differences in water purification of the basin in 2000, 2010, and 2020 well and provided a basis and scientific reference for the coordinated development and scientific planning of regional ecosystem security and water resources.

- The land use structure of the basin of two lakes and one reservoir showed arable land–forestland dominance. Arable land and forestland occupied an absolute dominant position, followed by construction land and grassland. unused land comprised the smallest proportion of the basin. From 2000 to 2020, only the area of construction land increased, and the areas of other land use types all decreased. From 2000 to 2020, the area of arable land in the basin decreased the most (by 185.37 km^2), and the area of construction land increased by 432.35 km^2.
- In 2000–2020, the total TN and TP export in the basin of two lakes and one reservoir did not change significantly, indicating that the water purification service of the basin in the 20 y from 2000 to 2020 had a small overall difference but obvious spatial differences. The high TN and TP export intensities were mainly distributed in the confluence area of the Dashiqiao River to the Maotiao River in the upstream area of the basin, on both banks of the Xinjiang River, and around the subbasin (where Hongfeng Lake is located) south of Qingzhen City, while the low TN and TP export intensities were mainly distributed in forestland.
- Of all land use types, forestland had the lowest TN and TP export per unit area, followed by grassland, indicating that forestland and grassland had the best water purification services. arable land had the highest TN and TP export per unit area. Additionally, arable land is an important source of nonpoint source pollution in the basin due to the great loss of N and P nutrients from fertilization and tillage.

Acknowledgments

This research was financially supported by the Natural Science Foundation of Guizhou Province (Qiankehe Foundation [2018]1418), the Science and Technology Support Project of Guizhou Province (Qiankehe Support [2018]2806 and [2020]4Y132), the Natural Science Foundation of Guizhou Province (Qiankehe Foundation [2020]1Y410).

References

[1] Y. Liu, X. Huang, H. Yang, T. Zhong, Environmental effects of land-use/cover change caused by urbanization and policies in Southwest China Karst area – a case study of Guiyang, Habitat Int., 44 (2014) 339–348.
[2] K. Arrow, B. Bolin, R. Costanza, P. Dasgupta, C. Folke, C.S. Holling, B.-O. Jansson, S. Levin, K.-G. Mäler, C. Perrings, D. Pimentel, Economic growth, carrying capacity, and the environment, Ecol. Econ., 15 (1995) 89–90.
[3] P.M. Vitousek, Beyond global warming: ecology and global change, Ecology Ecol. Soc. America, 75 (1994) 1861–1876.
[4] M.E. Assessment, Ecosystems and Human Well-Being: Synthesis, A Report of the Millennium Ecosystem Assessment, 2005, p. 534, doi: 10.1119/1.2344558.
[5] P.H. Verburg, K.-H. Erb, O. Mertz, G. Espindola, Land system science: between global challenges and local realities, Curr. Opin. Environ. Sustainability, 5 (2013) 433–437.
[6] C.Z. Sun, L.S. Zhao, W. Zou, D.F. Zheng, Water resource utilization efficiency and spatial spillover effects in China, J. Geog. Sci., 5 (2014) 771–788.
[7] S.B. Lu, Z.D. Lian, H.P. Sun, X.H. Wu, X. Bai, C.C. Wang, Simulating trans-boundary watershed water resources conflict, Resour. Policy, 73 (2021a) 102139, doi: 10.1016/j.resourpol.2021.102139.
[8] Z.X. Lu, Q. Feng, S.C. Xiao, J.L. Xie, S.B. Zou, Q. Yang, J.H. Si, The impacts of the ecological water diversion project on the ecology-hydrology-economy nexus in the lower reaches in an inland river basin, Resour. Conserv. Recycl., 164 (2021) 105154, doi: 10.1016/j.resconrec.2020.105154.
[9] Y.Y. Zhang, J. Xia, J.J. Yu, M. Randall, Y.C. Zhang, T.G. Zhao, X.Y. Pan, X.Y. Zhai, Q.X. Shao, Simulation and assessment of urbanization impacts on runoff metrics: insights from landuse changes, J. Hydrol., 560 (2018) 247–258.
[10] M.Y. Li, D. Liang, J. Xia, J.X. Song, D.D. Cheng, J.T. Wu, Y.L. Cao, H.T. Sun, Q. Li, Evaluation of water conservation function of Danjiang River Basin in Qinling Mountains, China based on InVEST model, J. Environ. Manage., 286 (2021a) 112212, doi: 10.1016/j.jenvman.2021.112212.
[11] Y.L. Lu, M.Y. Liu, S.Y. Zeng, C. Wang, Screening and mitigating major threats of regional development to water ecosystems using ecosystem services as endpoints, J. Environ. Manage., 293 (2021c) 112787, doi: 10.1016/j.jenvman.2021.112787.
[12] Y.L. Lu, J.J. Yuan, X.T. Lu, C. Su, Y.Q. Zhang, C.C. Wang, X.H. Cao, Q.F. Li, J.L. Su, V. Ittekkot, R.A. Garbutt, S. Bush, S. Fletcher, T. Wagey, A. Kachur, N. Sweijd, Major threats of pollution and climate change to global coastal ecosystems and enhanced management for sustainability, Environ. Pollut., 239 (2018) 670–680.
[13] H.G. Xiao, W. Ji, Relating landscape characteristics to non-point source pollution in mine waste-located watersheds using geospatial techniques, J. Environ. Manage., 82 (2007) 111–119.
[14] W. Ouyang, H.B. Huang, F.H. Hao, Y.S. Shan, B. Guo, Evaluating spatial interaction of soil property with non-point source pollution at watershed scale: the phosphorus indicator in Northeast China, Sci. Total Environ., 432 (2012) 412–421.
[15] C. Boix-Fayos, L.G.J. Boerboom, R. Janssen, M. Martínez-Mena, M. Almagro, P. Pérez-Cutillas, J.P.C. Eekhout, V. Castillo, J. Vente, Mountain ecosystem services affected by land use changes and hydrological control works in Mediterranean catchments, Ecosyst. Serv., 44 (2020) 101136, doi: 10.1016/j.ecoser.2020.101136.

[16] P. Hervé-Fernandez, C.E. Oyarzún, S. Woelfl, Throughfall enrichment and stream nutrient chemistry in small headwater catchments with different land cover in southern Chile, Hydrol. Processes, 30 (2016) 4944–4955.
[17] J. Xu, G.Q. Jin, H.W. Tang, P. Zhang, S. Wang, Y.-G. Wang, L. Lie, Assessing temporal variations of ammonia nitrogen concentrations and loads in the Huaihe River Basin in relation to policies on pollution source control, Sci. Total Environ., 642 (2018) 1386–1395.
[18] X.Y. Bai, W. Shen, P. Wang, X.H. Chen, Y.H. He, Response of non-point source pollution loads to land use change under different precipitation scenarios from a future perspective, Water Resour. Manage., 34 (2020) 3987–4002.
[19] W.Z. Wang, L. Chen, Z.Y. Shen, Dynamic export coefficient model for evaluating the effects of environmental changes on non-point source pollution, Sci. Total Environ., 747 (2020) 141164, doi: 10.1016/j.scitotenv.2020.141164.
[20] G.Q. Wang, J.W. Li, W.C. Sun, B.L. Xue, Y.L. A, T.X. Liu, Non-point source pollution risks in a drinking water protection zone based on remote sensing data embedded within a nutrient budget model, Water Res., 157 (2019) 238–246.
[21] Z.Y. Shen, X.S. Hou, W. Li, G. Aini, Relating landscape characteristics to non-point source pollution in a typical urbanized watershed in the municipality of Beijing, Landscape Urban Plann., 123 (2014) 96–107.
[22] K.A. Beckert, T.R. Fisher, J.M. O'Neil, R. Jesien, Characterization and comparison of stream nutrients, land use, and loading patterns in Maryland Coastal Bay Watersheds, Water Air Soil Pollut., 221 (2011) 255–273.
[23] M. Piaggio, J. Siikamäki, The value of forest water purification ecosystem services in Costa Rica, Sci. Total Environ., 789 (2021) 147952, doi: 10.1016/j.scitotenv.2021.147952.
[24] M.L. Mesnil, J.-B. Charlier, R. Moussa, Y. Caballero, N. Dörfliger, Interbasin groundwater flow: characterization, role of karst areas, impact on annual water balance and flood processes, J. Hydrol., 585 (2020) 124583, doi: 10.1016/j.jhydrol.2020.124583.
[25] M.G. Mostofa Amin, T.L. Veith, A.S. Collick, H.D. Karsten, A.R. Buda, Simulating hydrological and nonpoint source pollution processes in a karst watershed: a variable source area hydrology model evaluation, Agric. Water Manage., 180 (2016) 212–223.
[26] Z.K. Bargaoui, A. Chebbi, Comparison of two kriging interpolation methods applied to spatiotemporal rainfall, J. Hydrol., 365 (2009) 56–73.
[27] E.I. Nikolopoulos, M. Borga, J.D. Creutin, F. Marra, Estimation of debris flow triggering rainfall: influence of rain gauge density and interpolation methods, Geomorphology, 243 (2015) 40–50.
[28] M.F. Hutchinson, Interpolation of rainfall data with thin plate smoothing splines - Part I: two dimensional smoothing of data with short range correlation, J. Geogr. Inf. Decis. Anal., 2 (1998) 139–151.
[29] R.J. Hijmans, S.E. Cameron, J.L. Parra, P.G. Jones, A. Jarvis, Very high resolution interpolated climate surfaces for global land areas, Int. J. Climatol., 25 (2010) 1965–1978.
[30] D.T. Price, D.W. Mckenney, I.A. Nalder, M.F. Hutchinson, J.L. Kesteven, A comparison of two statistical methods for spatial interpolation of Canadian monthly mean climate data, Agric. For. Meteorol., 101 (2000) 81–94.
[31] H. Tallis, T. Ricketts, InVEST 1.0 Beta User's Guide: Integrated Valuation of Ecosystem Services and Tradeoffs, 2011.
[32] Y. Mei, X.H. Kong, X.L. Ke, B. Yang, The impact of cropland balance policy on ecosystem service of water purification—a case study of Wuhan, China, Water, 9 (2017) 1–12, doi: 10.3390/w9080620.
[33] Y.Y. Yan, Q.S. Guan, M. Wang, X.L. Su, G.J. Wu, P.C. Chiang, W.Z. Cao, Assessment of nitrogen reduction by constructed wetland based on InVEST: a case study of the Jiulong River Watershed, China, Mar. Pollut. Bull., 133 (2018) 349–356.
[34] W.C. Cong, X.Y. Sun, H.W. Guo, R.F. Shan, Comparison of the SWAT and InVEST models to determine hydrological ecosystem service spatial patterns, priorities and trade-offs in a complex basin, Ecol. Indic., 112 (2020) 106089, doi: 10.1016/j.ecolind.2020.106089.
[35] M. Nalej, Agricultural land cover changes in metropolitan areas of Poland for the period 1990–2012, Miscellanea Geographica, 20 (2016) 39–45.
[36] B.B. Wu, G.Q. Wang, H. Jiang, J.F. Wang, C.M. Liu, Impact of revised thermal stability on pollutant transport time in a deep reservoir, J. Hydrol., 535 (2016) 671–687.
[37] J. Yang, Y.D. Wang, S.Q. Fang, Y.F. Qiang, J.P. Liang, G.H. Yang, Y.Z. Feng, Evaluation of livestock pollution and its effects on a water source protection area in China, Environ. Sci. Pollut. Res., 27 (2020) 18632–18639.
[38] K.S. Bao, Y.F. Zhang, C. Zaccone, M.E. Meadows, Human impact on C/N/P accumulation in lake sediments from northeast China during the last 150 years, Environ. Pollut., 271 (2021) 116345, doi: 10.1016/j.envpol.2020.116345.
[39] C.C. Li, Y.P. Cai, Q. Tian, X. Wang, C.H. Li, Q. Liu, D.N. Chen, An integrated simulation-optimization modeling system for water resources management under coupled impacts of climate and land use variabilities with priority in ecological protection, Adv. Water Resour., 154 (2021b) 103986, doi: 10.1016/j.advwatres.2021.103986.
[40] Q. Longyang, Assessing the effects of climate change on water quality of plateau deep-water lake - a study case of Hongfeng Lake, Sci. Total Environ., 647 (2019) 1518–1530.
[41] M. Dalla Valle, E. Codato, A. Marcomini, Climate change influence on POPs distribution and fate: a case study, Chemosphere, 67 (2007) 1287–1295.
[42] B.J. Mahler, Y.J. Jiang, J.B. Pu, J. Martin, Editorial: advances in hydrology and the water environment in the karst critical zone under the impacts of climate change and anthropogenic activities, J. Hydrol., 595 (2021) 125982, doi: 10.1016/j.jhydrol.2021.125982.
[43] T.R. He, X.B. Feng, Y. Guo, G. Qiu, Z.G. Li, L. Liang, J.L. Lu, The impact of eutrophication on the biogeochemical cycling of mercury species in a reservoir: a case study from Hongfeng Reservoir, Guizhou, China, Environ. Pollut., 154 (2008) 56–67.
[44] X. Fang, Q. Wang, J.C. Wang, Y.Y. Xiang, Y.F. Wu, Y.F. Zhang, Employing extreme value theory to establish nutrient criteria in bay waters: a case study of Xiangshan Bay, J. Hydrol., 603 (2021) 127146, doi: 10.1016/j.jhydrol.2021.127146.
[45] J. Lyon, N.M. Gross, Patterns of plant diversity and plant–environmental relationships across three riparian corridors, For. Ecol. Manage., 204 (2005) 267–278.
[46] W. Wei, Y.N. Gao, J.C. Huang, J.F. Gao, Exploring the effect of basin land degradation on lake and reservoir water quality in China, J. Cleaner Prod., 268 (2020) 122249, doi: 10.1016/j.jclepro.2020.122249.